

Performance and Phase Change Kinetic Investigations on Capric-Myristic Acid Eutectic Mixtures for Energy-Saving Construction

Lin LI^{1,2}, Yu WANG^{1,2}, Xiaoming YU¹, Yanxia JI³, Mei-Ling ZHUANG^{4*}

¹ School of Architectural Engineering, Suqian College, Suqian 223800, China

² Jiangsu Province Engineering Research Center of Prefabricated Building and Intelligent Construction, Suqian 223800, China

³ School of Literature and Science, Suqian College, Suqian 223800, China

⁴ School of Transportation and Civil Engineering, Nantong University, Nantong, 226019, China

<http://doi.org/10.5755/j02.ms.34780>

Received 2 August 2023; accepted 18 October 2023

In the present study, capric acid and myristic acid were first selected to prepare a capric acid-myristic acid eutectic mixture using a compounding method. Then, the thermal properties, structural stability and weight loss of capric acid-myristic acid eutectic mixtures were analyzed using differential scanning calorimetry, Fourier transform infrared and thermogravimetry. Finally, the activation energy and reaction order of the capric acid-myristic acid eutectic mixture during solid-liquid transformation were calculated using the phase change kinetic methods of Kissinger and Ozawa. The results indicate that capric acid-myristic acid eutectic mixtures have good thermal cycle stability and stable energy storage in practical applications. The activation energies of capric acid-myristic acid eutectic mixtures were calculated using the phase change kinetic methods of Kissinger and Ozawa, with values of 345.6 kJ/mol and 333.3 kJ/mol, respectively, indicating that both phase change kinetic methods have good accuracy.

Keywords: thermal storage materials, capric acid, myristic acid, phase change kinetic.

1. INTRODUCTION

In recent years, energy has become increasingly scarce, seriously hindering economic and social development. How to develop and apply renewable energy sources and improve energy utilization has become an urgent issue [1]. Solar energy is a typical renewable energy source with the advantages of large storage capacity, wide distribution, cleanliness, and environmental protection [2]. It has attracted the attention and concern of various countries. However, its shortcomings, such as uneven radiation density, instability, and intermittency, also limit the continuous supply of energy [3]. To address this issue, scholars have proposed the use of latent heat storage technology to regulate, distribute and utilize solar energy to alleviate the mismatch in time and space [4]. Phase change materials, as the foundation and core of latent heat energy storage technology, have the characteristics of high energy storage density and nearly constant temperature during the phase change process, and can store or release energy at specific temperatures [5–7]. Latent heat energy storage technology utilizes this characteristic of PCMs to maintain a constant ambient temperature and compensate for energy imbalance [9].

Currently, PCM storage devices, such as collector systems, heating and cooling systems, and photovoltaic systems, are used in building energy efficiency applications to store solar energy [12, 13] and release energy when energy is scarce to ensure that these devices can work continuously around the clock. At present, PCMs have become an active research direction in the energy and

materials discipline [11]. PCMs are an effective means to alleviate energy crises and achieve sustainable energy utilization [12]. According to the changes in state during the phase change, PCMs can be divided into solid-solid PCMs, solid-gas PCMs, liquid-gas PCMs, and solid-liquid PCMs [13]. Solid-gas and liquid-gas PCMs are less commonly used because they produce gas during the phase change process, have large volume changes, and require complex equipment [14]. Solid-solid phase change materials do not have leakage problems because they have small volume changes and do not produce liquids or gases. Solid-liquid PCMs have received widespread attention due to their high heat storage density, wide phase change temperature range, and low price [15].

Fatty acids are widely used organic phase change materials, and their molecular formula can be expressed in general form as $\text{CH}_3(\text{CH}_2)_n\text{COOH}$. The latent heat of phase change of fatty acids is similar to that of alkanes with small super-cooling [16]. Fatty acids are ideal organic solid-liquid PCMs. Common fatty acid PCMs include lauric, myristic, and palmitic acids, as well as stearic and soft acids [17]. Fatty acids have the advantages of high latent heat of phase change, non-toxic and corrosion-free, and good thermal stability [18], while overcoming the disadvantages of inorganic PCM itself, such as being prone to supercooling or phase separation [19, 20]. The compound phase change temperature of fatty acids can satisfy the requirements of buildings, achieve indoor temperature fluctuations, improve comfort and save energy [19].

When evaluating the thermo-physical properties and thermal stability of new PCMs [21], macroscopic parameters and data after repeated thermal cycling are

* Corresponding author. Tel.: +86-18036558037;

fax: +86-0517-85374002. E-mail: ml_zhuang@ntu.edu.cn (M.L. Zhuang)

usually used to test the improvement of thermal storage capacity and stability performance of PCMs [22]. However, few studies have used microscopic phase change interface changes to analyze changes in thermal stability [23, 24]. Phase change kinetics can infer the changes in phase change energy of PCMs without repeated thermal cycling tests [25]. The thermal storage properties of CA and MA are closely related to the phase change behavior. Therefore, using phase transition kinetics to study the phase transition process of CA-MA eutectic mixtures can provide some theoretical basis for their practical applications.

In this article, capric acid (CA) and myristic acid (MA) were first selected to prepare CA-MA using a compounding method. Then, the thermal properties, structural stability and weight loss of CA-MA were analyzed through differential scanning calorimetry (DSC), Fourier transform infrared (FTIR) and thermogravimetry (TGA). Finally, the activation energy and reaction order of CA-MA during solid-liquid transformation were calculated using the phase change kinetic methods of Kissinger and Ozawa. The article is organized as follows. In Section 2, materials and test methods were presented. In Section 3, experimental results were analyzed and discussed from the thermal properties of CA, MA, CA-MA, structural stability and thermal decomposition stability of CA-MA. In Section 4, solid-liquid phase change kinetics of CA-MA were analyzed. In Section 5, the conclusions were drawn.

2. MATERIALS AND TEST METHODS FOR CA-MA

2.1. Materials and experimental instruments

1. Raw materials of CA-MA. Capric acid (CA, analytical purity, 98% pure) was produced by Shanghai Lingfeng Chemical Reagent Co. Ltd in China. Myristic acid (MA, analytical purity, 99% pure) was produced by Shanghai Aladdin Reagent Co. Ltd in China.
2. Experimental instruments. In this article, electronic balance JY2002, blast drying DGF30/14-IIA, differential scanning calorimeter (DSC) Netzsch DSC 200 F3, Fourier transform infrared (FTIR) Thermo Scientific Nicolet iN10, TGA Netzsch STA 449F5 were applied.

2.2. Test methods for CAMEM

2.2.1. Preparation of CA-MA

Two or more fatty acids can be mixed in any proportion and exhibit a high degree of compatibility, forming a minimum eutectic mixture with a specified phase transition temperature at the lowest eutectic point [26–28]. The phase change temperature of fatty acid PCMs is significantly reduced through compounding [27]. The compounding has high research value in low-temperature energy storage materials. The ratio of binary fatty acid eutectics and the corresponding latent heat of phase change and phase change temperature can be obtained as [29]:

$$\begin{cases} T_m = [1/T_i - (R \ln X_i) / H_i]^{-1} \\ H_m = T_m \cdot \sum_{i=1}^n \frac{x_i H_i}{T_i} \end{cases}, \quad (1)$$

where T_m is the melting point of eutectic mixture [30], and its unit is K; T_i is the melting point of the i th substance in the mixture, and its unit is K [31]; X_i is the molar percentage of the i th substance in the phase change mixture [31]; H_i and H_m are the latent heats of the i th substance and eutectic mixture, respectively, and its unit is J/mol [31]; R is the gas constant, which is 8.315 J/(mol·K) [32].

The two fatty acids were weighed in a container and heated until it was completely melted. After uniform mixing and cooling to room temperature, CA-MA can be obtained.

2.2.2. Thermal cycling test

Thermal cycling tests were carried out on CA-MA as follows. The phase change heat storage material was first placed in a tightly capped test tube. Then, the test tube was placed in a chamber resistance furnace at 100 °C for 10 minutes. The test tube was removed after the fatty acids CA and MA were completely mixed and melted. It was placed in an ice-water mixing vessel for 10 minutes to allow the acid eutectic mixtures to completely cool and solidify. The above step was one thermal cycle. The process was repeated to complete the corresponding number of thermal cycles. Finally, the relevant parameters of CA-MA samples were tested.

2.2.3. Analysis of the structure and properties

To obtain the phase change temperature and the latent heat of phase change of CA-MA samples, the DSC method was applied in this test. The sampling mass of DSC sample was 5 mg. Nitrogen was used as a protective gas. The scanning temperature range was -20.0 ~ 100.0 °C. The heating rates were set to 5.0 °C/min, 10.0 °C/min, 15.0 °C/min and 20.0 °C/min, respectively. Infrared spectroscopy was used to determine the compositional structure of the samples. The infrared spectrum of CA-MA samples was tested using the KBr compression method, with a scanning frequency of 400 ~ 4000 cm⁻¹. The mass loss of the sample at high temperature was determined by TGA. The scanning temperature range was 30.0 ~ 500.0 °C. The heating rate was 10 °C/min in the test.

2.3. Phase transformation dynamics

Kissinger [24] proposed the Kissinger method to analyze differential thermal analysis (DTA) curves. It can also be used to analyze DSC curves[33]. Its approximate equation is

$$\ln(\beta / T_p^2) = C - E_a / RT_p, \quad (2)$$

where β is the heating rate; T_p is the peak temperature of the DSC curve [33]; E_a is the apparent activation energy; R is the universal gas constant, 8.315 J/(K·mol); and C is a constant. The relationship between $\ln(\beta / T_p^2)$ and $1/T_p$ is linear. The apparent activation energy can be obtained from the slope [34].

Kissinger [35] proposed that the reaction order n can be calculated according to the peak shape index S :

$$\begin{cases} S = \frac{a}{b} \\ n = 1.26S^{1/2} \end{cases}, \quad (3)$$

where a and b are the vertical distances from the outer tangent of the curve inflection point to the peak.

The reliability and accuracy of the calculation results using the Kissinger method was verified by the Ozawa method [36]. The approximate equation is:

$$\lg \beta = C - 0.4567 E_a / RT_p \quad (4)$$

3. EXPERIMENTAL RESULTS AND DISCUSSION

3.1. Thermal properties

The molecular general formula of organic long-chain fatty acids is $\text{CH}_3(\text{CH}_2)_{2n}\text{COOH}$, where the carboxyl group is composed of a hydroxyl group and a carbonyl group, mainly affecting the chemical properties of fatty acids. Two fatty acid molecules combined with carbonyl oxygen and hydroxyl hydrogen to form bi-molecules, while the interlayer interaction relies on the weaker van der Waals forces. Through DSC tests, the thermal properties of monobasic fatty acids CA and MA were obtained in Table 1. The phase change temperatures (T) of CA and MA are 34.8 °C and 55.1 °C, respectively. Their latent heats of phase transition (LH) are 146.5 J/g and 175.7 J/g respectively. The phase change temperature of monobasic fatty acids CA or MA is higher than the comfort temperature range of the human body, so it can be used by compounding different types of fatty acids. In addition, the phase change temperature and latent heat of CA and MA gradually increases with the increase of molecular weight increase.

Table 1. Thermal properties of CA and MA

Name	Chemical formula	Molecular weight	T , °C	LH , J/g
CA	$\text{CH}_3(\text{CH}_2)_8\text{COOH}$	172.3	34.8	146.5
MA	$\text{CH}_3(\text{CH}_2)_{12}\text{COOH}$	228.4	55.1	175.7

3.2. Thermal properties

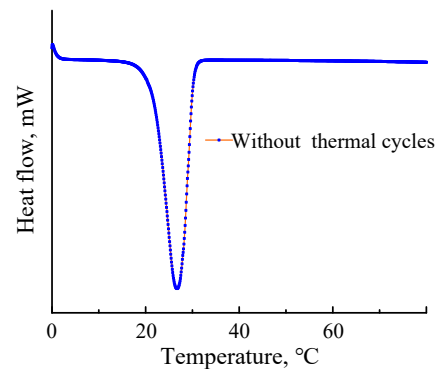
It is important to select the appropriate fatty acid PCMs within the required temperature range. Conducting theoretical predictions before conducting a large number of experiments can save costs and time, and provide some reference for the selection and application of PCMs. The phase change temperature and latent heat of CA and MA are brought into Eq. (1), it can be obtained $X_{\text{CA}} = 78.0\%$, $X_{\text{MA}} = 22.0\%$, $T_m = 297.5\text{ K}$ (24.4 °C) and $H = 146.6\text{ J/g}$. That is, CA-MA = 78:22 for CA-MA EM at 24.4 °C.

To obtain the thermal storage properties of CA-MA after the melting solidification process, CA-MA was subjected to 50 and 100 thermal cycles, respectively. The thermal properties of the phase change temperatures and latent heats with different thermal cycles were measured using DSC in Table 2. The values for T and LH of CA-MA are 21.7 °C and 156.7 J/g, respectively. Comparing the theoretical values with the test values, it can be found that the theoretical values meet the requirements of accuracy. The test values for T and LH of CA-MA with 50 thermal cycles are decreased by 1.4 % and 6.4 %, respectively. The test values of T and LH of CA-MA with 100 thermal cycles are decreased by 4.2 % and 4.7 %, respectively, performing

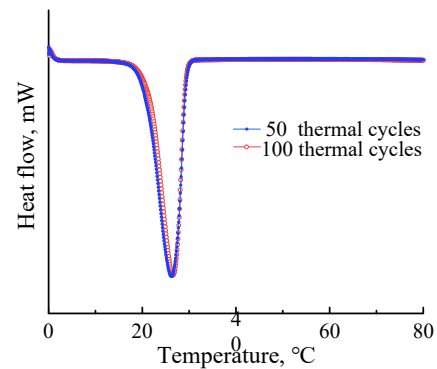
small changes within 100 thermal cycles and exhibiting good thermal cycle stability and reliability. Fig. 1 shows the DSC curves of CA-MA with different thermal cycles. After different repeated thermal cycling, the curves perform a single heat absorption peak, indicating that CA-MA does not appear as the phenomenon of the phase separation with different thermal cycles and can remain eutectic state.

Table 2. Thermal properties of CA-MA

Thermal cycles	T , °C	LH , J/g
Without thermal cycles	21.7	156.7
50 thermal cycles	21.4	146.7
100 thermal cycles	20.8	149.4



a



b

Fig. 1. DSC curves of CA-MA with and without thermal cycles: a – without thermal cycles; b – different thermal cycles

3.3. Structural stability

Fig. 2 gives the FTIR spectra of CA-MA with different thermal cycles. In Fig. 2, the C=O stretching vibration peak position of CA, MA and CA-MA without thermal cycles is 1700 cm^{-1} . The peak position of CA-MA with 100 thermal cycles is 1710.0 cm^{-1} . The in-plane bending vibrational absorption peak positions of the -OH group in mono acids and dibasic acids without thermal cycles are 1430.0 cm^{-1} . The out-of-plane bending vibrational absorption peak position of the -OH group in mono and dibasic acids without thermal cycles are 933.0 cm^{-1} and 941.0 cm^{-1} , respectively. The in-plane and out-of-plane vibrational absorption peak positions of the -OH group in CA-MA with 100 thermal cycles are 1420.0 cm^{-1} and 937.0 cm^{-1} , respectively. In the CA, MA and CA-MA without thermal cycles, the antisymmetric stretching vibration and symmetric stretching vibration peak positions of -CH₂ are 2920.0 cm^{-1} and 2850.0 cm^{-1} , respectively.

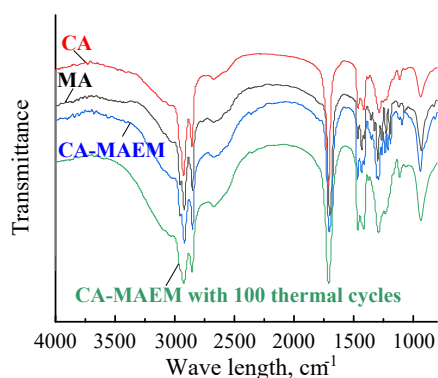


Fig. 2. FTIR spectra of the fatty acids

The peak position of the symmetric stretching vibration of $-\text{CH}_2$ in CA-MA is 2850.0 cm^{-1} after 100 thermal cycles. The infrared spectra of CA-MA without cycles and with 100 thermal cycling are consistent with those of the CA and MA. This indicates that the fatty acid molecules remain as dimers in CA-MA. After melt blending and thermal cycling of the fatty acids, the characteristic peaks of the main groups do not change significantly, and the peak shapes, positions and intensities are relatively stable with good structural stability. After compounding, no new peaks appeared in the binary acid compared to the single acid, indicating that the compounding did not produce new substances.

3.4. Thermal decomposition stability

The thermal decomposition stability of PCMs in the service environment is an important factor determining their long-term application as energy storage materials in building energy efficiency [37]. It is necessary to study the mass loss of CA-MA at high temperatures [37, 38]. The TGA analysis curves of CA-MA without thermal cycles and with 100 thermal cycles are all illustrated in Fig. 3.

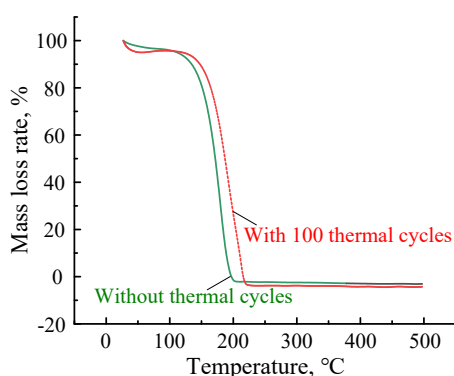


Fig. 3. TGA curves of CA-MA

At temperatures below $100.0 \text{ }^\circ\text{C}$, there is almost no mass loss of the two. both have almost no mass loss. The main weight loss temperature ranges of CA-MA without

Table 3. Thermal parameters of CA-MA with different heating rates

Heating rate, $^\circ\text{C}/\text{min}$	Initial temperature, $^\circ\text{C}$	Peak temperature, $^\circ\text{C}$	Terminal temperature, $^\circ\text{C}$	Latent heat, J/g	Heating rate, $^\circ\text{C}/\text{min}$
5	21.4	25.4	27.6	152.0	5
10	21.7	26.7	30.1	156.7	10
20	21.5	28.0	32.9	155.8	20
30	21.6	29.3	34.8	156.5	30

and with thermal cycles are $110.0 \sim 203.0 \text{ }^\circ\text{C}$ and $119.0 \sim 215.0 \text{ }^\circ\text{C}$, respectively. The temperature range required for PCMs in the construction field is about $15.0 \sim 40.0 \text{ }^\circ\text{C}$. Therefore, CA-MA can ensure good stability of thermal decomposition with and without thermal cycling.

4. SOLID-LIQUID PHASE CHANGE KINETICS

4.1. Phase change activation energy

Table 3 shows the thermal parameters of CA-MA with different heating rates. Fig. 4 shows DSC curves of CA-MA with different heat rates. In Fig. 4, each sample performs a single heat absorption peak. As the heating rate increases, the peak shape gradually shifts to the right, the peak temperature gradually increases, and the phase change temperature range also becomes larger.

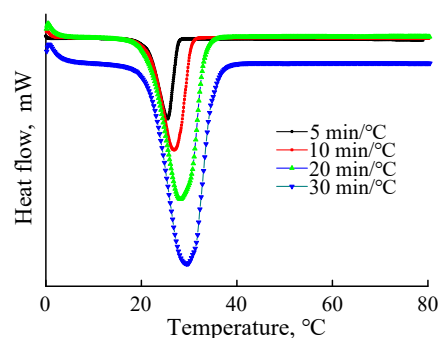


Fig. 4. DSC curves of CA-MA with different heating rates

The fitting curve of $\ln(\beta/T_p^2)-(1/T_p)$ is obtained using the Kissinger kinetic method, as shown in Fig. 5 a. The fitting curve of $\lg\beta-(1/T_p)$ is obtained by the Ozawa kinetic method, as shown in Fig. 5 b. Table 4 shows the activation energy values (E_a), correlation coefficient (R) values and the goodness of the fitting R^2 . Using the Kissinger method, the expression for the fitting curve of $\ln(\beta/T_p^2)$ is Eq. 5.

Using the Kissinger kinetic method, the apparent activation energy value E_a is 345.6 kJ/mol , the correlation coefficient R_c is -0.994 and the goodness of the fitting R_c^2 is 0.981 . Using the Ozawa method, the expression for the fitting curve of $\lg(\beta)$ is Eq. 6. Using the Ozawa method, the apparent activation energy value E_a is 333.3 kJ/mol , the correlation coefficient R is -0.994 and the goodness of the fitting R^2 is 0.981 .

$$\ln(\beta/T_p^2) = -41566.372(1/T_p) + 129.494; \quad (5)$$

$$\lg \beta = 62.051 - 18309.692(1/T_p). \quad (6)$$

Therefore, the phase change kinetic results obtained by the two processing methods are close to each other, their variation laws are the same, and their fitting accuracy is high.

Table 4. The kinetic analysis results of CA-MA using different kinetic methods

Kissinger kinetic method			Ozawa kinetic method		
E_a , kJ/mol	R_c	R_c^2	E_a , kJ/mol	R_c	R_c^2
345.60	-0.994	0.981	333.3	-0.994	0.981

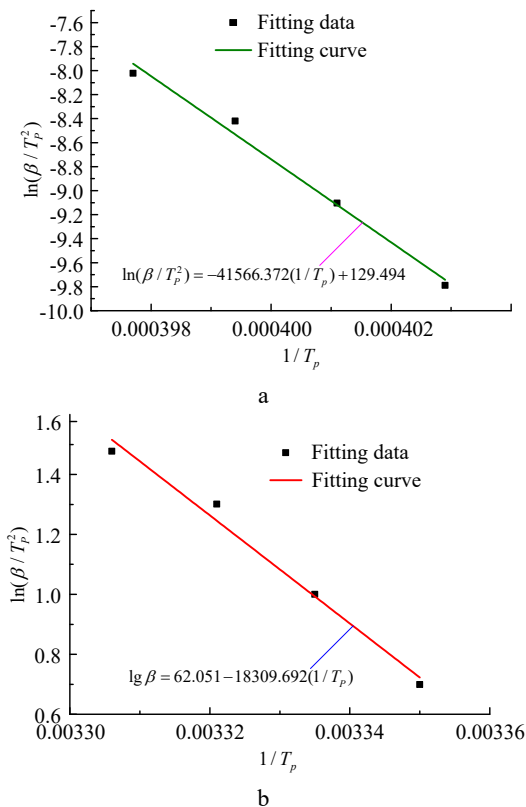


Fig. 5. Fitting curves using the two kinetic methods: a–Kissinger method; b–Ozawa method

4.2. Phase change reaction order

The solid-liquid phase change reaction orders with different heating rates can be obtained according to the solution method of reaction orders. Reaction orders of CA-MA with different heating rates are obtained in Table 5. The solid-liquid phase change reaction orders of CA-MA increase as the heating rate increases, which are all about 1.00.

Table 5. Reaction orders of CA-MA with different heating rates

Heating rate, °C/min	5.0	10.0	20.0	30.0
Reaction order n	0.99	1.02	1.03	1.05

5. CONCLUSIONS

In this article, CA and MA were prepared CA-MA by the compounding method. The thermal properties, structural stability and weight loss of CA-MA were analyzed and discussed by DSC, FTIR and TGA. The activation energy and reaction order of CA-MA during

solid-liquid transformation were calculated by different kinetic methods. The main conclusions are as follows:

1. The test values for T and LH of CA-MA are 21.7 °C and 156.7 J/g respectively. CA-MA can meet the requirements of energy-saving buildings.
2. CA-MA performs small and no significant fluctuations in phase change temperature and latent heat with 50 and 100 thermal cycles. It illustrates that CA-MA has good thermal cycle stability and stable energy storage in practical applications.
3. The activation energies calculated using Kissinger and Ozawa kinetic methods are 345.6 kJ/mol and 333.3 kJ/mol, respectively. The results calculated using the above two kinetic methods are relatively close, indicating that both kinetic methods have good accuracy.

Acknowledgments

This research has been supported by Suqian Science and Technology Program (Z2022099); and Suqian Top 1000 Talents Training Project in 2021.

REFERENCES

1. Liu, Z.J., Liu, Y.W., He, B.J., Xu, W., Jin, G.Y., Zhang, X.T. Application and Suitability Analysis of the Key Technologies in Nearly Zero Energy Buildings in China *Renewable Sustainable Energy Reviews* 101 2019: pp. 329–345. <https://doi.org/10.1016/j.rser.2018.11.023>
2. Li, M., Mu, B.Y. Fabrication and Characterization of Capric Acid/reduced Grapheme Oxide Decorated Diatomite Composite Phase Change Materials for Solar Energy Storage *Royal Society Open Science* 6 (1) 2019: pp. 181664. <https://doi.org/10.1098/rsos.181664>
3. Fu, X.W., Liu, Z.M., Wu, B., Wang, J.L., Lei, J.X. Preparation and Thermal Properties of Stearic Acid/diatomite Composites as Form-stable Phase Change Materials for Thermal Energy Storage via Direct Impregnation Method *Journal of Thermal Analysis and Calorimetry* 123 (2) 2016: pp. 1173–1181. <https://doi.org/10.1007/s10973-015-5030-1>
4. Song, M.J., Niu, F.X., Mao, N., Hu, Y.X., Deng, S.M. Review on Building Energy Performance Improvement using Phase Change Materials *Energy and Building* 158 2018: pp. 776–793. <https://doi.org/10.1016/j.enbuild.2017.10.066>
5. Liu, Y., Wang, M.Y., Cui, H.Z., Yang, L., Liu, J.P. Micro-/Macro-level Optimization of Phase Change Material Panel in Building Envelope *Energy* 195 (15) 2020: pp. 116932. <https://doi.org/10.1016/j.energy.2020.116932>
6. Wang, P.X., Feng, X.J., Zhu, Y.C., Lian, J.F., Zhang, H.Y., Fang, M. Preparation and Thermal Properties of Colloidal Mixtures of Capric Acid and $\text{Na}_2\text{HPO}_4 \cdot 12\text{H}_2\text{O}$ as a Phase Change Material for Energy Storage *Solar Energy Materials and Solar Cells* 215 2020: pp. 11036.
7. Sweidan, A.H., Heider, Y., Markert, B. Modeling of PCM-based Enhanced Latent Heat Storage Systems using a Phase-field-porous Media Approach *Continuum Mechanics and Thermodynamics* 32 2020: pp. 861–882. <https://doi.org/10.1007/s00161-019-00764-4>

8. **Chen, Z.R., Yao, X.M., Yin, X.P.** Preparation of Kaolin based Phase Change Thermal Storage Materials for Solar Thermal Power Plant *Renewable Energy Resources* 37 (3) 2019: pp. 349–353.
<https://doi.org/10.3969/j.issn.1671-5292.2019.03.006>
9. **Rao, Z.H., Xu, T.T., Liu, C.Z., Zheng, Z.J., Liang, L., Hong, K.** Experimental Study on Thermal Properties and Thermal Performance of Eutectic Hydrated Salts/Expanded Perlite Form-stable Materials for Passive Solar Energy Utilization *Solar Energy Materials and Solar Cells* 188 2018: pp. 6–17.
<https://doi.org/10.1016/j.solmat.2018.08.012>
10. **Mahfuz, M.H., Anisur, M.R., Kibria, M.A., Saidur, R., Metselaar, I.H.S.C.** Performance Investigation of Thermal Energy Storage System with Phase Change Material (PCM) for Solar Water Heating Application *International Communications in Heat and Mass Transfer* 57 2014: pp. 132–139.
<https://doi.org/10.1016/j.icheatmasstransfer.2014.07.022>
11. **Zhao, L., Xing, Y.M., Liu, X., Luo, Y.G.** Thermal Performance of Sodium Acetate Trihydrate Based Composite Phase Change Material for Thermal Energy Storage *Applied Thermal Engineering* 143 2018: pp. 172–181.
<https://doi.org/10.1016/j.applthermaleng.2018.07.094>
12. **Gu, Q.J., Fei, H., Wang, L.Y., Fang, M., Jiang, D.H., Zhao, Y.C.** Phase Transition Properties of Capric Acid-hexadecanol as Phase Change *Chemical Industry and Engineering Progress* 38 (11) 2019: pp. 5033.
<https://doi.org/10.16085/j.issn.1000-6613.2019-0335>
13. **Cabeza, L.F., Castell, A., Barreneche, C., Gracia, A.D., Fernandez, A.** Materials Used as PCM in Thermal Energy Storage in Buildings: A Review *Renewable & Sustainable Energy Reviews* 15 (3) 2011: pp. 1675–1695.
<https://doi.org/10.1016/j.rser.2010.11.018>
14. **Xiao, Q.Q.** Preparation, Properties and Application in Solar Water Heating System of Light-to-thermal Conversion Phase Change Materials. Doctoral dissertation. South China University of Technology, China, 2020.
15. **Diarce, G., Quant, L., Campos-Celador, A., Sala, J.M., Garcia-Romero, A.** Determination of the Phase Diagram and Main Thermophysical Properties of the Erythritol-urea Eutectic Mixture for Its Use as a Phase Change Material *Solar Energy Materials and Solar Cells* 157 2016: pp. 894–906.
<https://doi.org/10.1016/j.solmat.2016.08.016>
16. **Li, M., Kao, H.T., Wu, Z.S., Tan, J.M.** Study on Preparation and Thermal Property of Binary Fatty acid and the Binary Fatty *Applied Energy* 88 2011: pp. 1606–1612.
17. **Zhang, W.Y., Zhang, X.G., Huang, Z.H., Yin, Z.Y., Wen, R.L., Huang, Y.T., Wu, X.W., Min, X.** Preparation and Characterization of Capric-palmitic-stearic Acid Ternary Eutectic Mixture/Expanded Vermiculite Composites as Form-stabilized Thermal Energy Storage Materials *Journal of Materials Science & Technology* 34 2018: pp. 379–386.
<https://doi.org/10.1016/j.jmst.2017.06.003>
18. **Karthikeyan, K., Mariappan, V., Kalidoss, P., Anish, R., Sarfoji, P., Janke, V.R., Tapas, K.S.** Preparation and Thermal Characterization of Capric-myristic Acid Binary Eutectic Mixture with Silver-antimony Tin Oxide and Silver-graphane Nanoplatelets Hybrid-nanoparticles as Phase Change Material for Building Applications *Materials Letters* 328 2022: pp. 133086.
<https://doi.org/10.1016/J.MATLET.2022.133086>
19. **Sari, A., Kaygusuz, K.** Some Fatty Acids Used for Latent Heat Storage: Thermal Stability and Corrosion of Metals with Respect to Thermal Cycling *Renewable Energy* 28 2003: pp. 939–48.
[https://doi.org/10.1016/S0960-1481\(02\)00110-6](https://doi.org/10.1016/S0960-1481(02)00110-6)
20. **Shen, Q., Jing, O.Y., Zhang, Y., Yang, H.M.** Lauric acid/Modified Sepiolite Composite as a Form-stable Phase Change Material for Thermal Energy Storage *Applied Clay Science* 146 2017: pp. 14–22.
<https://doi.org/10.1016/j.clay.2017.05.035>
21. **Zayed, M.E., Zhao, J., Elsheikh, A.H., Du, Y.P., Hammad, F.A., Ma, L.** Kabeel A. E., Sadek S. Performance Augmentation of Flat Plate Solar Water Collector Using Phase Change Materials and Nanocomposite Phase Change Materials: A Review *Process Safety and Environmental Protection* 128 2019: pp. 135–157.
<https://doi.org/10.1016/j.psep.2019.06.002>
22. **Parameshwaran, R., Sari, A., Jalaiah, N., Karunakaran, R.** Applications of Thermal Analysis to the Study of Phase-Change Materials *Handbook of Thermal Analysis and Calorimetry* 6 2018: pp. 519–572.
<https://doi.org/10.1016/B978-0-444-64062-8.00005-X>
23. **Xu, T., Chen, Q.L., Huang, G.S., Zhang, Z.G., Gao, X.N., Lu, S.S.** Preparation and Thermal Energy Storage Properties of D-Mannitol/Expanded Graphite Composite Phase Change Material *Solar Energy Materials and Solar Cells* 155 2016: pp. 141–146.
<https://doi.org/10.1016/j.solmat.2016.06.003>
24. **Zhang, H.G., Zhu, J.Q., Cheng, X.M., Zhou, W.B., Liu, F.L.** Effect of Modified Vermiculite on the Interface of a Capric Acid-expanded Vermiculite Composite Phase Change Material with Phase Transition Kinetics *Journal of Wuhan University of Technology (Material Science)* 148 (2) 2019: pp. 91–98.
<https://doi.org/10.1007/s11595-019-2058-2>
25. **Luo, Z.G., Zhang, H., Gao, X.N., Xu, T., Fang, Y.T., Zhang, Z.Z.** Fabrication and Characterization of Form-stable Capric-palmitic-stearic Acid Ternary Eutectic Mixture/Nano-SiO₂ Composite Phase Change Material *Energy and Buildings* 147 2017: pp. 41–46.
<https://doi.org/10.1016/j.enbuild.2017.04.005>
26. **Eanest, J.B., Valan, A.A.** Characterisation and Stability Analysis of Eutectic Fatty Acid as a Low Cost Cold Energy Storage Phase Change Material *Journal of Energy Storage* 31 2020: pp. 101708.
<https://doi.org/10.1016/j.est.2020.101708>
27. **Yuan, Y.P., Zhang, N., Tao, W.Q., Cao, X.L., He, Y.L.** Fatty Acids as Phase Change Materials: A Review *Renewable and Sustainable Energy Reviews* 29 2014: pp. 482–498.
<https://doi.org/10.1016/j.rser.2013.08.107>
28. **Ke, H.Z., Pang, Z.Y., Peng, B., Wang, J., Cai, Y.B., Huang, F.L., Wei, Q.F.** Thermal Energy Storage and Retrieval Properties of Form-stable Phase Change Nanofibrous Mats Based on Ternary Fatty Acid Eutectics/Polyacrylonitrile Composite by Magnetron Sputtering of Silver *Journal of Thermal Analysis and Calorimetry* 123 (2) 2016: pp. 1293–1307.
<https://doi.org/10.1007/s10973-015-5025-y>
29. **Zhang, Y.P., Su, Y.H., Ge, X.S.** Eutectic Phase Change Material Melting Point and the Prediction of the Heat of Fusion Theory *Journal of University of Science and Technology of China* 25 (4) 1995: pp. 475–476.
<https://doi.org/CNKI:SUN:ZKJD.0.1995-04-016>

30. **Du, W.Q., Fei, H., He, Q., Wang, L.Y., Pan, Y.C., Liu, J.T.** Preparation and Properties of Capric Acid–stearic acid-based Ternary Phase Change Materials *RSC Advances* 11 2021: pp. 24938. <https://doi.org/10.1039/D1RA03925C>
31. **Zhang, N., Yuan, Y.P., Li, T.Y., Cao, X.L., Yang, X.J.** Study on Thermal Property of Lauric–palmitic–stearic Acid/Vermiculite Composite as Form-stable phase Change Material for Energy Storage *Advances in Mechanical Engineering* 7 (9) 2015: pp. 1–8. <https://doi.org/10.1177/1687814015605023>
32. **Lv, P.Z., Liu, C.Z., Rao, Z.H.** Review on Clay Mineral-based Form-stable Phase Change Materials: Preparation, Characterization and Applications *Renewable and Sustainable Energy Reviews* 68 2017: pp. 707–726. <https://doi.org/10.1016/j.rser.2016.10.014>
33. **Wu, K.Z., Li, J.L., Zhang, J.J., Liu, X.D.** Nonisothermal Kinetics of the Solid-Solid Phase Transitions in the Perovskite Type Layer Compounds $(C_nH_{2n+1}NH_3)_2ZnCl_4$ *Chinese Journal of Chemistry* 26 2008: pp. 216–219. <https://doi.org/10.1002/cjoc.200890027>
34. **Gao, J.G., Jiang, C.J., Zhang, X.J.** Kinetics of Curing and Thermal Degradation of POSS Epoxy Resin/DDS System *International Journal of Polymeric Materials* 56 (1) 2007: pp. 65–77. <https://doi.org/10.1080/00914030600710620>
35. **Kissinger, H.E.** Reaction Kinetics in Differential Thermal Analysis *Analytical Chemistry* 29 1957: pp. 1702–1706.
36. **Ozawa, T.** Kinetic Analysis of Derivative Curves in Thermal Analysis *Journal of Thermal Analysis* 2 1970: pp. 301–324. <https://doi.org/10.1007/bf01911411>
37. **Zhang, X.G., Huang, Z.H., Yin, Z.Y., Zhang, W.Y., Huang, Y.T., Liu, Y.G., Fang, M.H., Wu, X.W., Min, X.** Form Stable Composite Phase Change Materials from Palmitic-lauric Acid Eutectic Mixture and Carbonized Abandoned Rice: Preparation, Characterization, and Thermal Conductivity Enhancement *Energy and Buildings* 154 2017: pp. 46–54. <https://doi.org/10.1016/j.enbuild.2017.08.057>
38. **Xue, H., Cui, Y.D., Zhang, B.N., Guo, Q.Y., Feng, G.Z.** Preparation and Properties of Capric-Lauric-Palmitic Acid Eutectic Mixtures/Expanded Graphite Composite as Phase Change Materials for Energy Storage *Advanced Materials Research* 1028 2014: pp. 40–45. <https://doi.org/10.4028/www.scientific.net/AMR.1028.40>



© Li et al. 2024 Open Access This article is distributed under the terms of the Creative Commons Attribution 4.0 International License (<http://creativecommons.org/licenses/by/4.0/>), which permits unrestricted use, distribution, and reproduction in any medium, provided you give appropriate credit to the original author(s) and the source, provide a link to the Creative Commons license, and indicate if changes were made.